

Non Ideal Instabilities in Field Reversed θ -Pinches

M.A.M. SANTIAGO, A.S. GOMES

Instituto de Física, Universidade Federal Fluminense, Niterói, 24210, RJ, Brasil

and

P.H. SAKANAKA

Instituto de Física Gleb Wataghin, Universidade Estadual de Campinas, Caixa Postal 1170, Campinas, 13100, SP, Brasil

Recebido em 4 de novembro de 1986; versão revista em 8 de maio de 1987

Abstract Rotational Instabilities and resistive tearing modes are the most striking modes observed in high temperature O-pinches with zero or reversed bias field. We study these configurations which have the effect of a rigid rotation of the plasma column. Some recent experimental data indicate that an $m=2$ mode appears after the rotation reaches a critical value. We show that the growth rate of the $m=2$ mode may be greater than that of the $m=1$ resistive kink mode, depending on the experimental conditions. We apply our results to several experimental data in the literature.

1. INTRODUCTION

The purpose of this work is to extend the paper by Galvão and Santiago¹ to include the $m=2$ tearing mode in field reversed O-pinches. In this paper we considered the $m=1$ kink instability in those configurations including a rigid rotation of the plasma column to explain some theoretical and experimental data given in the literature^{2,3,4,5}. In this case an anti-parallel bias magnetic field is applied before the initial compression field, so that a configuration of closed field lines is produced which inhibits particle losses. The resistive tearing mode expected in these configurations is analysed in the limit of long wavelength and rigid rotation. A rotational instability is the most striking mode observed in high temperature O-pinches and provides one of the main limitations to confinement. Usually an $m=2$ mode grows and the plasma, firstly rotating as a rigid body, becomes elliptical and, in many cases, breaks up into two filaments, rotating about each other. In some conditions however an $m=1$ mode predominates. This is less well understood

Work partially supported by FINEP, CNEN, CNPq and CAPES (Brazilian Government Agencies).

but is also associated with the rotation². Mechanisms to explain the origin of the rotation have been reviewed by Haines² and it is probable that more than one mechanism takes place in practice. In the latter reference, rotation due to a small transverse field was observed during the implosion phase and the ions were found to carry a substantial fraction of current, as expected.

The fundamental question in these instabilities is, firstly, the fact that in many situations the $m=2$ mode is observable but in other cases the $m=1$ kink mode is the dominant mode. We also remark that higher modes ($m \geq 2$) are rarely observed and the absence of these modes suggests the presence of some damping or stabilising mechanism³.

The $m=1$ instability appears to be associated with the rotation but there is no satisfactory theory to account for the observations⁴. In recent studies³ the frequency and wavelength of the instability were found to agree with theory and the rotation could be explained by observed end shorting currents and involved the propagation of a torsional Alfvén wave inwards along the column. We see that more work is needed, particularly experiments with new diagnostics to fully explain both the $m=1$ and $m=2$ modes, the rotational instability is still a serious limitation in theta pinches with zero or reversed bias field.

In our system we consider a plasma cylindrical layer whose thickness is small compared with its radius, with the magnetic field in opposite directions on either side of it. We show that the growth rate of the $m=2$ mode scales with the $1/3$ power of the plasma resistivity and the frequency of the mode is given by

$$\omega = 2\Omega + i\Lambda \left(\frac{\tau_H}{\tau_R} \right)^{1/3} \tau_H^{-1} \quad (1)$$

where the Alfvén hydromagnetic characteristic time is given by

$$\tau_H = (kV_A)^{-1} ,$$

where

$$V_A = B / (4\pi\rho)^{1/2} ,$$

$$\tau_R = 4\pi r_0^2 / \eta c^2$$

the resistive diffusion time, η the plasma resistivity, k the longitudinal mode number, and r , the radius where the magnetic field vanishes. In presence of a finite resistivity η , magnetic field lines diffuse through the plasma and the rate is proportional to the time scale defined by τ_R . Simple resistive diffusion is generally much slower than the ideal ($\eta=0$) plasma response defined by τ_H , but special field configurations can give rise to much more rapid diffusion. This magnetic reconnection consists in the growth of one or more regions in terms of the total magnetic flux in the region at the expense of other regions. The reconnection time is given by $\tau = S^p \tau_H$ where $S = \tau_R / \tau_H$ is the Lundqvist number and p depends on the self-consistent geometry, magnetic field and boundary conditions, varying from zero to one. In present fusion research devices $S \approx 10^7$, so the reconnection rates vary greatly depending on the value of p . In eq. (1) Λ represents a scalar quantity of order unity, and it appears in the eigenvalue equation that will be obtained in section 2.

Our main result is that the growth rate of the $m=2$ mode is greater than that of the $m=1$ resistive tearing mode previously studied¹, depending on the experimental data of the magnetic field configuration. Actually, one of the most important problems on the confinement of a field reversed configuration plasma produced by reversed field O-pinch is to suppress this $m=2$ rotational instability^{6,7}. Recently this has been obtained by using a quadrupole field⁸.

A basic difference between our work and previous work on resistive instabilities lies in that in our case the parallel component of fluid displacement is much larger than the radial component in the resistive layer, leading the plasma column to breakup into separate rings. We apply our results to several experimental data in the literature and, as usual using MHD theory, some quantitative results differ one order of magnitude from the observed ones; our better results are concentrated on modes where the resistivity effect is predominant.

2. EQUILIBRIUM AND PERTURBED EQUATIONS

We use MHD equations including rotation of the plasma column in equilibrium. Our basic equations are:

$$\rho \frac{d\vec{V}}{dt} = \frac{1}{4\pi} (\nabla \times \vec{B} \times \vec{B}) - \nabla p \quad , \quad (2)$$

$$\frac{\partial \vec{B}}{\partial t} = \nabla \times (\vec{V} \times \vec{B}) - \nabla \times \left(\frac{\eta c^2}{4\pi} \nabla \times \vec{B} \right) \quad , \quad (3)$$

$$\nabla \cdot \vec{B} = 0 \quad , \quad \text{and} \quad \nabla \cdot \vec{V} = 0 \quad . \quad (4)$$

Here ρ , \vec{B} , $\vec{V} = r\Omega\hat{\theta}$, and p represent, respectively, the mass density, magnetic field, fluid velocity and pressure in equilibrium. The profile of B is represented in fig. 1. The resistivity is small in sense that the characteristic times are much shorter than the resistive diffusion time. The basic equation in equilibrium, neglecting the resistivity, is:

$$\frac{\Omega^2 a^2}{V_A^2} f(\bar{r}) = \frac{d}{d\bar{r}} (\beta + b^2) \quad (5)$$

where $f = \rho/\bar{\rho}$, $\beta = 8\pi p/\bar{B}^2$, $\bar{r} = r^2/a^2$, \bar{B} and $\bar{\rho}$ being the average values of B and ρ , a the radius of the plasma column, $b = B/\bar{B}$ and $V_A^2 = \bar{B}^2/4\pi\bar{\rho}$. We also assume that the equilibrium variables are only dependent on r .

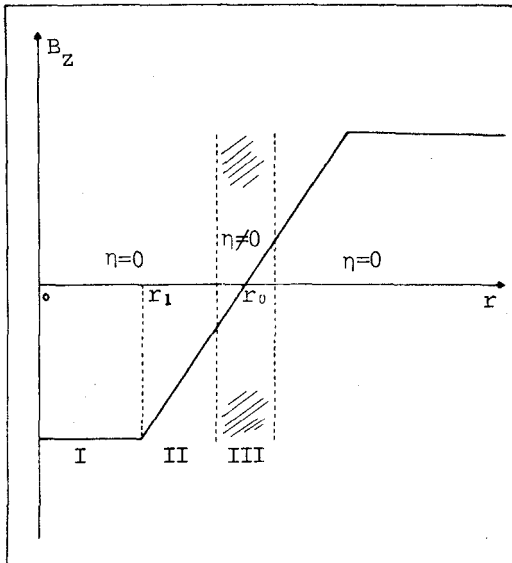


Fig.1 - Configuration of the Reversed Equilibrium Magnetic Field.

We do not include other dissipative effects such as viscosity, because the modes described in this paper are driven unstable by the magnetic field energy presented in field reversed configurations, and this energy can be tapped only through the finite plasma resistivity.

Following the same previous treatment we consider a small region around the point r_0 where $B=0$ and inside it we take into account η and R . The solutions of the layer or resistive equations are asymptotically matched to the ones of the external or ideal equations ($\eta=0$) and we calculate the growth rate of the modes.

We linearize eqs. (2)-(4) and assume perturbations of the form

$$\tilde{\chi} = \chi_1(r) \exp[i(-\omega t + m\theta + kz)]$$

and obtain

$$\nabla \times \left[\frac{\partial \vec{V}}{\partial t} + \rho_0 \vec{V}_0 \cdot \nabla \vec{V}_1 + \rho_0 \vec{V}_1 \cdot \nabla \vec{V}_0 + \rho_1 \vec{V}_0 \cdot \nabla \vec{V}_0 \right] = \frac{1}{4\pi} \nabla \times (\vec{B}_0 \cdot \nabla \vec{B}_1 + \vec{B}_1 \cdot \nabla \vec{B}_0) \quad (6)$$

$$\frac{\partial \vec{B}_1}{\partial t} = \nabla \times [(\vec{V}_0 \times \vec{B}_1) + (\vec{V}_1 \times \vec{B}_0)] + \nabla \times \left(\frac{\eta c^2}{4\pi} \nabla \times \vec{B}_1 \right) \quad , \quad (7)$$

$$\nabla \cdot \vec{B}_1 = 0 \quad , \quad \text{and} \quad \nabla \cdot \vec{V}_1 = 0 \quad (8)$$

where the subscripts 0 and 1 refer, respectively, to the equilibrium and perturbed quantities.

Our analysis of the resistive and ideal equations follows the general treatment for the m modes developed in previous papers^{1,5}.

Defining the small parameter $\epsilon \equiv \tau_H/\tau_R \ll 1$ we scale the resistive equations¹ to obtain the eigenvalue equation. Using the set eqs. (6)-(8) we obtain for the components of the perturbed quantities

$$-i\omega(\omega - m\Omega) \rho \left(\frac{m}{r} \xi_z - k\xi_\theta \right) - 2\omega\Omega \rho k \xi_r + \omega k \rho_0 r \frac{d\Omega}{dr} \xi_r = \frac{1}{4\pi} \left(-m \frac{k}{r} B B_{1z} + \right. \\ \left. + i \frac{m}{r} \frac{dB}{dr} B_{1r} + k^2 B B_{1\theta} \right) \quad , \quad (9)$$

$$\begin{aligned}
 & -i(\omega - m\Omega) (k\rho\xi_r + i \frac{d}{dr} (\rho\xi_z)) - 2\omega\Omega\rho k\xi_\theta + i\omega\Omega \frac{\Omega kr}{\omega - m\Omega} \frac{d\rho}{dr} \xi_r - m\omega\rho_0 \frac{d\Omega}{dr} \xi_z = \\
 & = \frac{1}{4\pi} \left[k^2 B B_{1r} + \frac{d}{dr} (ik B B_{1z} + \frac{dB}{dr} B_{1r}) \right] , \tag{10}
 \end{aligned}$$

$$\begin{aligned}
 & -\omega(\omega - m\Omega) \left(\frac{1}{r} \frac{d}{dr} (r\rho\xi_\theta) - i \frac{m}{r} \rho\xi_r \right) - 2i\omega\Omega \frac{1}{r} \frac{d}{dr} (\rho r\xi_r) + m\omega\rho_0 \frac{d\Omega}{dr} \xi_\theta \\
 & + 2\omega\Omega\rho \frac{m}{r} \xi_\theta - i\omega\Omega \frac{m\Omega}{\omega - m\Omega} \frac{d\rho}{dr} \xi_r - 2i\omega\rho_0 \frac{d\Omega}{dr} \xi_r - i\omega \frac{d\Omega}{dr} \frac{d}{dr} (\rho_0 r\xi_r) \\
 & - i\omega\rho_0 \frac{d}{dr} (r \frac{d\Omega}{dr}) \xi_r = \frac{1}{4\pi} \left(\frac{1}{r} \frac{d}{dr} (ikr B B_{1r}) + \frac{mk}{r} B B_{1r} \right) , \tag{11}
 \end{aligned}$$

$$(\omega - m\Omega) B_{1r} = ik B \omega \xi_r + \frac{i\eta}{4\pi} \left[\frac{1}{r} \frac{d}{dr} (r \frac{dB}{dr} B_{1r}) - \frac{m^2 + 1 + k^2 r^2}{r^2} \times B_{1r} - 2i \frac{m}{r^2} B_{1\theta} \right] \tag{12}$$

$$\begin{aligned}
 (\omega - m\Omega) B_{1\theta} = ik B \omega \xi_r = ik B \omega \xi_\theta + \frac{i\eta}{4\pi} \left[\frac{1}{r} \frac{d}{dr} (r \frac{dB}{dr} B_{1\theta}) - \frac{m^2 + 1 + k^2 r^2}{r^2} B_{1\theta} \right. \\
 \left. + \frac{2im}{r^2} B_{1r} \right] + ir \frac{d\Omega}{dr} B_{1r} , \tag{13}
 \end{aligned}$$

and

$$(\omega - m\Omega) B_{1z} = ik B \omega \xi_z - \omega \frac{dB}{dr} \xi_r + \frac{i\eta}{4\pi} \left[\frac{1}{r} \frac{d}{dr} (r \frac{dB}{dr} B_{1z}) - \frac{m^2 + k^2 r^2}{r^2} B_{1z} \right] \tag{14}$$

where $\vec{\xi} = \int \vec{V}_1 dt$ and $\sigma = \omega - m\Omega$.

The ideal equation, taking the limit of large wavelength,

$$k^2 r^2 \ll m^2 ,$$

is:

$$\begin{aligned}
 \frac{d}{dr} \left[r^3 \left(\rho_0 \sigma^2 - \frac{k^2 B^2}{4\pi} \right) \right] \frac{d\xi_r}{dr} + r \left[-(\rho_0 \sigma^2 - \frac{k^2 B^2}{4\pi}) (m^2 - 1) + \right. \\
 \left. + r \frac{d}{dr} \left(\rho_0 \omega^2 - \frac{k^2 B^2}{4\pi} \right) \right] \xi_r = 0 \tag{15}
 \end{aligned}$$

The width of the layer is defined by $\delta = \epsilon^b$ and a is given by

$$\sigma = i\epsilon^a \Lambda \tau_H^{-1} ; \Lambda \sim \Theta(1) \tag{16}$$

We scale the perturbed variables as:

$$\begin{aligned} B_{1r} &= -i \left[kr_0 \left(r \frac{dB}{dr} \right) r_0 \frac{\omega}{\sigma} \right] \epsilon^c \psi_r \\ B_{1\theta} &= -i \left[kr_0 \left(r \frac{dB}{dr} \right) r_0 \frac{\omega}{\sigma} \right] \epsilon^d \psi_\theta \\ B_{1z} &= -i \left[kr_0 \left(r \frac{dB}{dr} \right) r_0 \frac{\omega}{\sigma} \right] \epsilon^e \psi_z \end{aligned} \tag{17}$$

$$\xi_r = r_0 \hat{\xi}_r ; \xi_\theta = r_0 \epsilon^f \hat{\xi}_\theta ; \xi_z = r_0 \epsilon^g \hat{\xi}_z ,$$

where

$$\hat{\xi}_r \sim \hat{\xi}_\theta \sim \hat{\xi}_z \sim \psi_r \sim \psi_\theta \sim \psi_z \sim \Theta(1).$$

In the ordering of the resistive equations we require that terms that vanish when $\eta \rightarrow 0$ become of order unity. This is consistent with the choice

$$a = b = c = \frac{1}{3} ; d = e = 0 ; f = g = -\frac{1}{3}$$

With this choice we can see that

$$\xi_z / \xi_r \sim B_{1z} / B_{1r} \sim \epsilon^{-1/3} \gg 1$$

We can see that the parallel component of the fluid displacement is much larger than the radial component in the layer, and the plasma column tends to break up into thin and elongated helical islands.

Taking the limit $k^2 r^2 \ll m^2$, supposing a rigid rotation ($d\Omega/dr=0$) and using the appropriated scaling, the set of resistive equations has a well known solution⁵ and there is an asymptotic solution that behaves as

$$\xi_{r'} \sim \frac{1}{X} \Big|_{X \rightarrow \infty} \quad \text{and} \quad \hat{\xi}_{r'} = c^{te} = \xi_{\infty} \quad ; \quad X = (r-r_0)/\delta r_0.$$

We show in the appendix that the field equation for the $m = 2$ mode has a solution that behaves as $\hat{\xi}_{\text{MHD}} = A(1 + \frac{C}{x})$ when $x \rightarrow 0$

$$x = (r-r_0)/r_0 = \delta X \quad .$$

Thus the asymptotic matching with the resistive equations can be made by using the relation

$$\left(\frac{1}{A} \frac{d\hat{\xi}_{\text{MHD}}}{dx} \right)_{x \rightarrow 0} = \left(\frac{1}{\xi_{\infty}} \frac{d\hat{\xi}_{r'}}{dX} \right)_{X \rightarrow \infty} \quad (18)$$

Using the solutions given by Coppi et al.⁵ and the corresponding one in the appendix we obtain the eigenvalue equation

$$F(\Lambda) = \Lambda^{5/4} \frac{\Gamma[(\Lambda^{3/2} - 1)4]}{\Gamma[(\Lambda^{3/2} + 5)4]} = \frac{8}{\pi} \epsilon^{1/3} e^{-1} \quad (19)$$

with h given by eq.(16).

C is determined by matching the ideal equation outside the layer and depends on the model of the magnetic field configuration. This is shown in the appendix for the $m = 2$ mode.

We find h from the values of ϵ which are calculated by using the experimental data.

3. ANALYSIS OF THE EXPERIMENTAL RESULTS

We apply our calculations firstly to the three cases of experimental data given by Eberhagen and Grossmann⁹ to obtain C , for the $m=1$ and $m=2$ modes, and consequently, the ratio R given by eq. (A.8). The quantities $R_{\tilde{\nu}}$ for these three cases are shown in figure 2 as functions of $(-x_1)$. We also show in this figure the eigenvalues $\Lambda_{\tilde{\nu}}$ for $m=2$. The quantity $s = x_1 r_0 / \tilde{b}_{\infty}$, where r_0 and $\tilde{b}_{\infty} = -B(r=0)/B_{\infty}$ were taken as constant, represents the inverse slope of the magnetic field profile. So, given x_1 we can calculate the eigenvalue h and then the growth rate for a given slope. We show in figure 2 that the $m=2$ mode is dominant over the

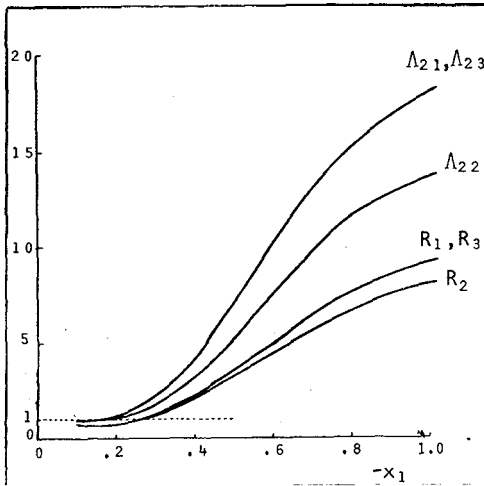


Fig.2 - Profiles of the eigenvalues Λ_i for $m=2$, and the ratio R_i between the eigenvalues for $m=2$ and $m=1$ for the data of Eberhagen and Grossmann⁹, for $r_{0i} = 1.1, 1.0$ and 1.4 cm and $s = 0.33, 0.67$ and 0.35 cm, respectively. The subscript i refers to the three cases described in this experiment.

$m=1$ mode for $(-x_1) > 0.3$. For the experimental data used we calculate $(-x_1) \sim 0.10$, and $\gamma \sim 0.37 \times 10^6 \text{ s}^{-1}$ for the $m=1$ mode.

Experimental observations indicate that the $m=1$ mode introduces an annular structure, stable for times of the order of $10 \mu\text{s}$. In these experiments the times associated to the growth of the mode are given by $\tau_{\text{exp}} > 13 \mu\text{s}$ and $\tau_{\text{exp}} > 9 \mu\text{s}$. We consider only lower limits, because the time is measured from the beginning of the deformation to the onset of the rotational instability.

This is consistent with the fact that the $m=2$ mode is not observed in this experiment, for any value of the rotation frequency. With our results the theoretical time is of the order of $2.7 \mu\text{s}$.

Recently Minato *et al.*⁸ stabilized the $m=2$ rotational mode in a field reversed configuration (FRC) produced by a field reversed Θ -pinch by the application of the quadrupole field. This mode was studied by several authors and the multipole-field suppression is now common^{10,11}. A high β FRC plasma of $T_i \approx 300 \text{ eV}$, $T_e = 100 \text{ eV}$ and $n_e = 2.7 \times 10^{15} \text{ cm}^{-3}$ with a radius equal to 3.5 cm and 60 cm of length, was confined by an axial magnetic field of 0.8 T . Without the quadrupole field, the $m = 2$ rotational instability induces an elliptic deformation of the plasma column with an angular frequency of $0.85 \times 10^6 \text{ s}^{-1}$. Applying the present

theory for these experimental data, with $(-x_1) = 0.4$, we find $\Lambda_2 = 6.4$ and $\gamma = 0.46 \times 10^6 \text{ s}^{-1}$. The reconnection time associated is found to be $\tau = 2.2 \mu\text{s}$.

Without the quadrupole field the $m=2$ mode occurs $15 \mu\text{s}$ after the plasma production and grows up to the time of $35 \mu\text{s}$ when the plasma collapses. We represent in figure 3 the ratio R for this experiment and the experiments of Pharos and the Julietta device at Jülich² are represented in figure 4.

In the Pharos experiment, with a dense plasma ($n = 10^{23} \text{ m}^{-3}$) and spectroscopically determined electron temperatures of up to about 900 eV, studies of the rotational instability were carried out. The confinement time of about $12 \mu\text{s}$ indicated a rapid loss process and this was attributed either to the rotational instability or to end losses associated with the instabilities at the end of the closed field line system. We apply our results to this case and find for $(-x_1) = 0.40$, $\gamma_2 = 0.25 \times 10^6 \text{ s}^{-1}$ and a reconnection time of $3.9 \mu\text{s}$.

In the Jülich experiment, the rotational instability was also observed and detailed studies of axial structure were carried out, this is consistent with the resistive tearing mode. In this experiment, with $T \sim 150 \text{ eV}$, $B_0 \sim 18 \text{ kG}$, $B_\infty = 31 \text{ kG}$ the observed growth rate was of the order of $1.1 \mu\text{s}$. Applying our theory we calculate for $(-x_1) = 0.40$, $\Lambda_2 = 10.4$, $\gamma_2 \sim 0.98 \times 10^6 \text{ s}^{-1}$, and the reconnection time associated $\sim 1.0 \mu\text{s}$.

4. CONCLUSIONS

We have studied the $m=2$ resistive mode in reversed field configurations. The most important result is that its growth rate may be greater than the one of the $m=1$ resistive kink mode, depending on the experimental conditions. Thus, this mode may be associated to the splitting of the plasma column in an annular structure as it is observed in tearing modes. The most important problem in the confinement of FRC plasma produced by field reversed O-pinch is to suppress the $m=2$ rotational instability. We show for an experiment in which this mode is

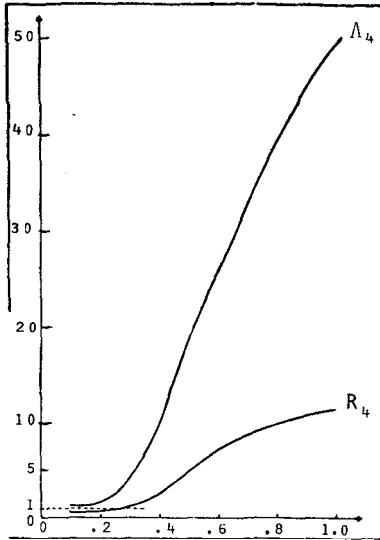


Fig.3 - Profiles of the eigenvalue Λ_n for $m=2$ and the ratio R_4 between the eigenvalues for $m=2$ and $m=1$ for the data of Minato et al.⁷.

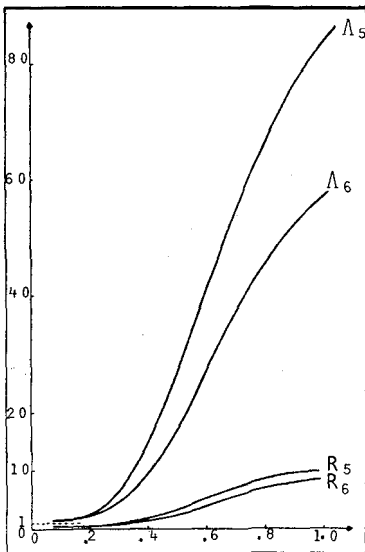


Fig.4 - Profiles of the eigenvalues Λ_n , for $m=2$ and the ratio R_n between the eigenvalues for $m=2$ and $m=1$ for the data of Pharos and Jülich².

suppressed by applying a quadrupole field, it would lead the plasma to collapse in a time of $2 \mu s$, one order of magnitude less than the measured time. The difference may be due to the limitations of the MHD theory such as the lack of finite Larmor radius effects or to the effect of a Doppler shift in the mode frequency due to rotation.

For a more realistic treatment we probably need to change the boundary layer model by a global method that extends the plasma resistivity to all the region of plasma. We are now performing the continuation of this approach and then we will be able to obtain the explicit effect of the rotation in the imaginary part of the eigenfrequency. Consequently, the modes we have studied are pure resistive tearing modes. Our better quantitative result is concentrated in the Julietta device and this implies that the resistive effect is predominant in this experiment. Linear theory offer a limited version of the tearing mode behaviour. The first non linear effect occurs when the size of the island exceeds the corresponding one of the tearing layer and in this case non linear currents dominate the inertia.

The authors are grateful for the comments by Dr. R.M.O.Galvão, Dr. K.H.Tsui, and to Prof.C.A.Azevedo for useful discussions.

APPENDIX

In this appendix we solve the ideal MHD eq.(15) for the $m=2$ mode. We neglect in this equation the terms $\rho_0 \sigma^2$ and make the change of variable $x = (r-r_0)/r_0$. The two linearly independent solutions, for region II of figure 1, are of the form

$$\xi_{r_1} = (1+x)F(a, b, c; -x) \tag{A.1}$$

where F is the hypergeometric function with $a = 3 - \sqrt{5}$, $b = 3 + \sqrt{5}$ and $c = 2$ and

$$\xi_{r_2} = (1+x)F(a, b, c; -x) \ln(-x) + (1+x) \sum_{n=1}^{\infty} \frac{(a)_n (b)_n}{(c)_n n!} (-x)^n |\psi_n| - \frac{1+x}{x} \tag{A.2}$$

where

$$|\psi_n| = \Delta\psi_n(a) + \Delta\psi_n(b) - \Delta\psi_n(c) - \Delta\psi_n(1) \quad ,$$

with

$$\Delta\psi_n(k) = \psi(k+n) - \psi(k) \quad ,$$

and

$$(z)_n = \frac{\Gamma(z+n)}{\Gamma(z)} \quad ; \quad \psi(z) = \Gamma'(z)/\Gamma(z)$$

The general solution for region II is

$$\xi_{r_{II}} = A\xi_{r_1} + B\xi_{r_2} \quad (A.3)$$

When

$$x \rightarrow 0 \quad ; \quad \xi_{r_{II}} \sim A(1 + \frac{C}{x}) \quad ; \quad C = -B/A \quad (A.4)$$

The general solution for region I is

$$\xi_{r_I} = A * r \quad (A.5)$$

We determine the constant C by matching the two solutions at the boundary point $x_1 = (r_1 - r_0)/r_0$,

$$\xi_{r_I} = \xi_{r_{II}} \Big|_{x=x_1} \quad (A.6)$$

and

$$\xi_{r_I}' = \xi_{r_{II}}' \Big|_{x=x_1}$$

where the prime denotes derivative with respect to x .

Thus the eigenvalue is calculated by eq. (19) and the growth rate of the mode is given by

$$\sigma = \omega - 2\Omega = i \epsilon^{1/3} \Lambda \tau_H^{-1} = i\gamma$$

The growth rate scales with $\eta^{1/3}$, since

$$\varepsilon \sim \tau_R^{-1} = \frac{\eta e^2}{4\pi x_0}$$

The solution of eq. (A.6) gives

$$C = - \frac{\xi_{r_1} - (1 + x_1) \xi_{r_1}'}{\xi_{r_2} - (1 + x_1) \xi_{r_2}'}$$

We can see that plasma rotation introduces a Doppler shift in the mode frequency. The ratio between the growth rates of the $m = 1$ and $m = 2$ modes, γ_1 and γ_2 , is given by

$$R = \frac{\gamma_2}{\gamma_1} = \frac{\Lambda_2}{\Lambda_1} \quad (\text{A.8})$$

since $\gamma_i = \varepsilon^{1/3} \Lambda_i \tau_H^{-1}$, $i = 1$ or 2 .

We developed a simple numerical code that calculates $C(-x_1)$; $0 < (-x_1) < 1$, with the solutions ξ_{r_1} and ξ_{r_2} , and the left side of eq.(19) for several values of A . ε is determined from experimental values of the magnetic field, density and temperature (for calculating τ_H and τ_R). Consequently for each point $(-x_1)$ and for fixed ε we can determine the eigenvalue A for both $m = 1$ and $m = 2$ modes.

REFERENCES

1. R.M.O.Galvão and M.A.M.Santiago, Phys.Fluids 24(4), 661 (1981).
2. H.A.Bodin, *High Beta Linear Devices*, Culham Laboratory Rev. Report ch.4, to be published.
3. J.P.Freidberg and L.D.Pearlstein; Phys.Fluids 21, 1207 (1978).
4. E.Bowers and M.G.Haines, Phys.Fluids 14, 165 (1971).
5. B.Coppi et al, Fiz.Plazmy 2, 1961 (1976).
6. T.Ishimura, Institute of Plasma Physics, Nagoya University, Research Report IPPJ - 608 (1982).

7. D.J.Rey, W.T.Armstrong, G.A.Barnes, R.E.Chriea, W.N.Hugrass, P.L. Klingner, K.F.McKenna and M.Tuszewski, Phys.Fluids 29,2648 (1986).
8. T.Minato *et al.*, Proc. fo the 9th International Conference on Plasma Physics and Controlled Nuclear Fusion Research (Baltimore) IAEA - CN 41/M-3 (1982).
9. A.Eberhagen and W.Grossmann, Z.Phys. 248, 130 (1971).
10. Ohi *et al.*, Phys. Rev. Lett. 51, 1042 (1983).
11. A.L.Hoffman, J.T.Slough and D.G.Harding, Phys.Fluids 26, 1626 (1983).

Resumo

Modos resistivos de rompimento e instabilidades rotacionais são os mais relevantes modos observados em O-pinches de alta temperatura com ou sem campo reverso de polarização. Estudamos estas configurações como efeito de uma rotação rígida da coluna de plasma. Alguns dados experimentais mais recentes indicam que um modo $m=2$ aparece depois que a rotação alcança um valor crítico. Mostramos que a taxa de crescimento do modo $m=2$ pode ser maior que a do modo resistivo de dobra $m=1$ dependendo das condições experimentais. Aplicamos nossos resultados a diversos dados experimentais encontrados na literatura.